Application of the Lattice Boltzmann Method to the Acoustic Wave in a Rectangular Enclosure

Jaouad Benhamou[1] [a], Mohammed Jami[1] [b] and Ahmed Mezrhab[1]

[1]*Mechanics & Energetics Laboratory, Faculty of Sciences, Mohammed First University, 60000 Oujda, Morocco.*

Abstract: An application of the lattice Boltzmann method (LBM) to the study of sound wave propagation is presented in this paper. The major purpose of this simulation is to show how the LBM technique can be easily applied in the domain of acoustics. The sound waves are emitted from a vibrating rectangular source placed in the center of the left face of a rectangular enclosure filled with air. An analytical study is performed to validate our numerical approach and the error between the two studies is also described to ensure the validity of the LBM analysis.

1 INTRODUCTION

The history of the LBM method stems from two different approaches, the kinetic theory of discrete velocity distribution gases and lattice gases (Bechereau, 2017). The first approach is generally used to model a system composed of a large number of particles such as a gas using statistical description tools (Mohamad, 2011; Timm et al, 2017; Tristani, 2015). A lattice gas is a cellular automaton developed to simulate the behaviour of a fluid (Frisch et al., 1986; McNamara and Zanetti, 1988). That is, a structured grid of cells. Each of these cells is in a state (empty or full) which evolves over time.

The application of the LBM in different scientific fields has been well known in the literature for a long time. This numerical method is a mesoscopic approach that can simulate various physical mechanisms such as fluid flows, wave propagation and heat transfer. For example, for wave simulation, the LBM has been employed for many years to study many types of waves such as elastic (Frantziskonis, 2011; O'Brien et al., 2012), sound (Benhamou et al., 2020; Buick et al., 1998; Salomons et al., 2016), aeroacoustic (Marié et al., 2009; Weidong and Jun, 2019) and shock waves (Guangwu et al., 1999; Xiao, 2007).

In this article, our work deals with numerical and analytical studies of the sound waves propagation. For numerical simulation, the LB method is used to model the waves produced using the point source modelling tool. In the analytical case, the study will be carried out using the mathematical expression of cylindrical waves given by the resolution of the standing wave equation.

It is important to mention that the study of sound waves is chosen in this article as a research topic because its applications are very important in various fields, especially in the industrial (Moudjed, 2013) and medical (Ranganayakulu et al., 2016; Sarvazyan et al., 2013) sectors.

2 NUMERICAL APPROACH

For the LBM simulations, there are two popular models to simulate different physical problems: multiple relaxation time (MRT) and single relaxation time (SRT) models. In the case of acoustic wave simulation, the MRT model is more stable and precise than the SRT scheme (Viggen, 2009). For this simple reason, the LBM-MRT model is chosen in this work to simulate the wave propagation. In this way, the description of the fluid evolution using this model can be given by the following discrete Boltzmann

[a] https://orcid.org/0000-0002-1958-2843

[b] http://orcid.org/0000-0002-5356-4729

equation (Mohamad, 2011; Benhamou et al., 2020; Jami et al., 2016; Mezrhab et al., 2010):

$$f_i(x_i + c_i \Delta t, t + \Delta t) - f_i(x_i, t) = M^{-1} S[m_i^{eq} - m_i] \quad (1)$$

where f_i represents the distribution function in direction i, c_i denotes the velocities of the lattice used, Δt is the time step, S is the relaxation matrix and M^{-1} is the inverse matrix of the transformation matrix M. m_i and m_i^{eq} are the fluid moments and equilibrium moments, respectively.

The discretization of the velocity space allows to define the LBM lattice. Therefore, it is necessary to choose a set of well reduced velocities to optimize the computation time of the LBM simulations. However, the number of velocities must be sufficient to describe the dynamic behaviour of the flow and the velocities should not be chosen randomly. The choice of the LBM lattice is therefore very important. Generally, it is necessary to choose a symmetrical lattice in order to obtain the flow behaviour at the macroscopic scale. Usually, the D2Q9-LBM scheme (Figure 1) is employed to determine the macroscopic quantities such as velocities and density (Mohamad, 2011).
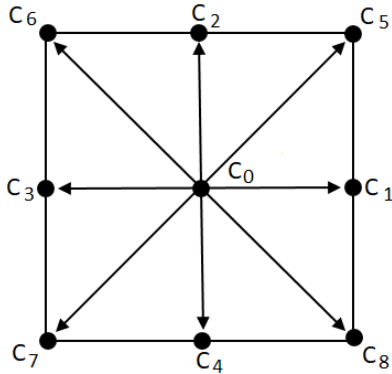

Figure 1: The D2Q9-LBM model.

The matrix S is a diagonal matrix. In this LBM simulation, the nine relaxation rates are the same as those mentioned in the references (Mohamad, 2011; Benhamou et al., 2020):

$$S = \text{diag}(1, 1.4, 1.4, 1, 1.2, 1, 1.2, s_7, s_8) \quad (2)$$

The two relaxation rates s_7 and s_8 are equal and related to the kinematic viscosity (ν) as:

$$s_7 = s_8 = \frac{1}{3\nu + 0.5} \quad (3)$$

The matrices M and M^{-1} are matrices (9*9). Their role is to map the nine distribution functions to the space of moments:

$$m = Mf \quad \text{and} \quad f = M^{-1}m \quad (4)$$

The mathematical expression of the M is given as (Mohamad, 2011):

$$M =$$
$$\begin{pmatrix}
1 & 1 & 1 & 1 & 1 & 1 & 1 & 1 & 1 \\
0 & 1 & 0 & -1 & 0 & 1 & -1 & -1 & 1 \\
0 & 0 & 1 & 0 & -1 & 1 & 1 & -1 & -1 \\
-4 & -1 & -1 & -1 & -1 & 2 & 2 & 2 & 2 \\
4 & -2 & -2 & -2 & -2 & 1 & 1 & 1 & 1 \\
0 & -2 & 0 & 2 & 0 & 1 & -1 & -1 & 1 \\
0 & 0 & -2 & 0 & 2 & 1 & 1 & -1 & -1 \\
0 & 1 & -1 & 1 & -1 & 0 & 0 & 0 & 0 \\
0 & 0 & 0 & 0 & 0 & 1 & -1 & 1 & -1
\end{pmatrix} \quad (5)$$

The moment vector m is given as a function of the density, physical energy, energy flux, impulsion and the physical quantities related to the components of the stress tensor (Benhamou et al., 2020; Mezrhab et al., 2010).

The vector m_i^{eq} depends of the fluid density and the macroscopic velocities (u, v) (Mohamad, 2011).

$$
\begin{aligned}
m_0^{eq} &= \rho \\
m_1^{eq} &= -2\rho + 3\rho^2(u^2 + v^2) \\
m_2^{eq} &= \rho - 3\rho^2(u^2 + v^2) \\
m_3^{eq} &= \rho u \\
m_4^{eq} &= -\rho u \\
m_5^{eq} &= \rho v \\
m_6^{eq} &= -\rho v \\
m_7^{eq} &= \rho^2(u^2 - v^2) \\
m_8^{eq} &= \rho^2 uv
\end{aligned}
\quad (6)
$$

Differently from CFD methods, which are based on solving the differential equations, the LBM is a statistical approach that gives the macroscopic quantities as the mean of the microscopic quantities outlined by the functions f_i. For example, for the D2Q9 schema, the density (ρ) and velocities (u, v)) can be computed as (A. A. Mohamad, 2011):

$$\rho = \sum_{i=0}^{8} f_i, \quad \rho u = \sum_{i=0}^{8} f_i \, c_i \quad \text{and} \quad \rho v = \sum_{i=0}^{8} f_i \, c_i \quad (7)$$

where c_i are the nine LBM velocities of the D2Q9 model.

3   BOUNDARY CONDITIONS

The boundary conditions applied at all walls of the rectangular enclosure are the bounce-back boundary conditions (BBC). These types of conditions are typically employed to rebound the fluid particles at the solid boundaries. The BBC are based on the idea

that the known functions can be exploited at the boundaries to determine the unknown functions. For example, an implementation of the BBC at the vertical walls of a rectangular cavity is illustrated in figure 2. At the west boundary, the functions f_1, f_5 and f_8 are respectively replaced by f_3, f_7, f_6. At the east wall, the functions f_3, f_6 and f_7 are given as follows: $f_3 = f_1$, $f_6 = f_8$ and $f_7 = f_5$.

Figure 2: Illustration of the Bounce-back boundary conditions.

4   RESULTS AND DISCUSSION

The geometry of the physical problem is depicted in figure 3. The sound waves are emitted by a vibrating rectangular source placed in the center of the left wall of a rectangular enclosure filled with air. The acoustic source is discretized into a set of point sources based on the acoustic point source technique (Benhamou et al., 2020; Salomons et al., 2016; Viggen, 2009). This technique allows the sound waves to be easily produced. For a single point source, the waves can be described by the following equation:

$$\rho = \rho_0 + \rho_A \, sin \left(\frac{2\pi t}{T}\right) \qquad (8)$$

where the parameters ρ_A, t, T and ρ_0 represent the amplitude, the time, the period, and the equilibrium density ($\rho_0 = 1$), respectively.

It should be noted that this model is only valid in cases of weak oscillations, i.e. in cases where the amplitude is very small compared to the equilibrium density ($\rho_0 \gg \rho_A$) (Viggen, 2009).

For the point source, it is necessary to confirm that it behaves in a way that corresponds to the analytical solution of the simulated physical problem. In 2D, the emitted acoustic waves are the circular waves corresponding to the cylindrical waves in 3D (Salomons et al., 2016; Viggen, 2009). Thus, the analytical solution can be expressed as:

$$\rho = A H_0^{(2)}(kr)e^{j\frac{2\pi}{T}t} \qquad (9)$$

where A is a constant, $H_0^{(2)}$ is the Hankel function, which depends on the wave number k and the

distance to the source r. All the parameters represented in this equation (Equation (9)) are well discussed in the references (Benhamou et al., 2020; Viggen, 2009).
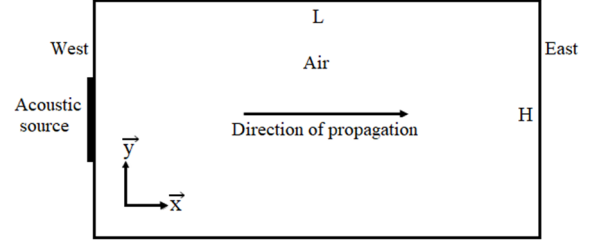

Figure 3: Simulated physical problem.

It should be noted that our LBM code has already been validated by comparing our results obtained from a single acoustic source placed in the center of a square air-filled cavity. This validation is illustrated in reference (Benhamou et al., 2020). It is reported on the simulation of circular wave propagation in air at time 1600 and for a period and viscosity of 40 and 0.06, respectively.

The numerical results obtained for this simulation are given in figure 4 . From this figure, it can be seen that the waves produced are plane and propagating in the x-direction towards the right wall of the enclosure. These waves are obtained by the interference of circular waves emitted by discrete acoustic point sources. This result are obtained at 700 iterations ($t = 700$). At this time, the waves arrive at the east wall and begin to be reflected by this boundary.

The diameter of the rectangular source considered here is H/3, it corresponds to 100 point sources for a mesh of 400*300 nodes. The priode (T) is equal to 40, the viscosity (ν) is fixed at 0.02 and the amplitude (ρ_A) is chosen in a way that the acoustic model used always remains linear ($\rho_A = 0.01$) (Benhamou et al., 2020).
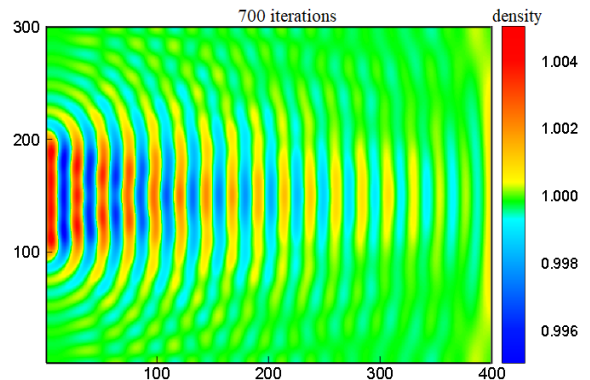

Figure 4: Simulation results of the acoustic waves propagation in enclosure filled with air at 700 iterations.

To further validate our numerical results, the analytical analysis results are also presented in this work. As mentioned previously, for a single acoustic source, this analytical solution is given by equation (9). In the case of the source shown in figure 3, the analytical solution is given by the sum of the density fields of the point acoustic sources.

The mathematical expression of the constant A appearing in equation (9) can be expressed as (Viggen, 2009) :

$$A = a\, \rho_A\, e^{-\frac{j2\pi}{3}} \qquad (10)$$

where a is a constant and ρ_A is the amplitude of the point source. The factor a depends in particular on the viscosity used. For example, for a LBM period of 20, the values of a found by Viggen (Viggen, 2009) for viscosities of 0.166 and 0.033 are 0.135 and 0.15, respectively.

It is worth noting that the mathematical expression of A (equation (10)) is given from a comparison of the analytical and numerical results (Viggen, 2009). The analytical resolution of equation (9) gives an analytical solution very close to the numerical results found. However, there is a discrepancy (gap) between these two solutions. This is due to the term $e^{-j2\pi/3}$ expressed in equation (10). This gap can be clearly seen in figure 5, which represents the analytical and numerical longitudinal profiles of the density along the x-axis at time 700 and at the position H/2. The calculation of the absolute error (Ea) is also presented. This error can be determined as the difference between the analytical (ρ_{Anl}) and numerical (ρ_{Num}) densities (Benhamou et al., 2020):

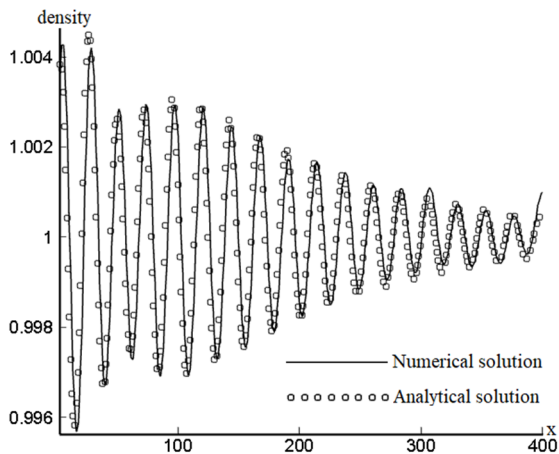$$Ea = \left| \rho_{Anl} - \rho_{Num} \right| \qquad (11)$$

Figure 5: Longitudinal profiles of the numerical and analytical densities along the x-axis given by equations (8) and (9) in the presence of the constant A expressed in equation (10).

Figure 6 illustrates the variation of Ea along the x-axis. It fluctuates between 0 and $2.22\ 10^{-3}$ very close to the rectangular sound source and its variation becomes small away from the source. It should be noted that for the maximum value found in this calculation ($2.22\ 10^{-3}$), the error can be considered significant in relation to the variation of the density, which oscillates between 0.996 and 1.004 (see Figure 5). Consequently, the analytical solution must be improved.
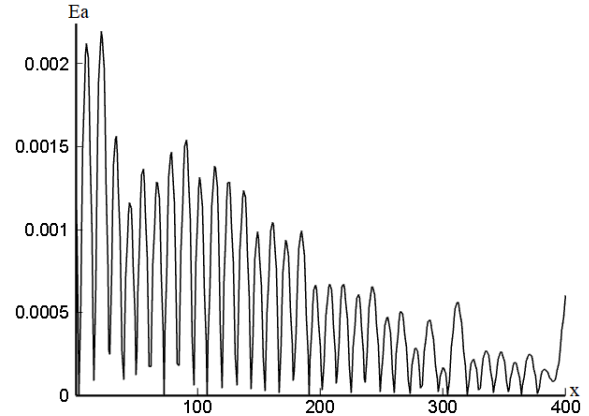

Figure 6: Fluctuation of the absolute error between the analytical and numerical densities along the x-axis.

Many tests have been performed to improve the gap between analytical and numerical results, i.e. to improve the absolute error. We found very good agreement between the two results if equation (10) becomes:

$$A = a\, \rho_A\, e^{-\frac{j\pi}{2}} \qquad (12)$$

It is important to note that the absolute value of the density obtained by using this last expression is high compared to that found by using equation (10) and therefore it leads to the improvement of the absolute error between the numerical and analytical results. The change of the mathematical expression of the constant A is tested in the present studied configuration and will be tested in other subsequent work. The new results found are shown in figure 7. A good correspondence between the analytical and numerical calculations can be seen from this figure.

As for the first case, the absolute error (Ea) is calculated and is depicted in figure 8. From this figure, it can be seen that Ea varies between 0 and about $4.5\ 10^{-4}$ along the x-axis, except in the vicinity of the acoustic source and the right wall of the cavity where it takes a more significant value. The maximum value of Ea ($8\ 10^{-4}$) can be considered very low compared to its former maximum value

($2.22 \ 10^{-3}$) which indicates that the numerical results are now very close to those calculated analytically.
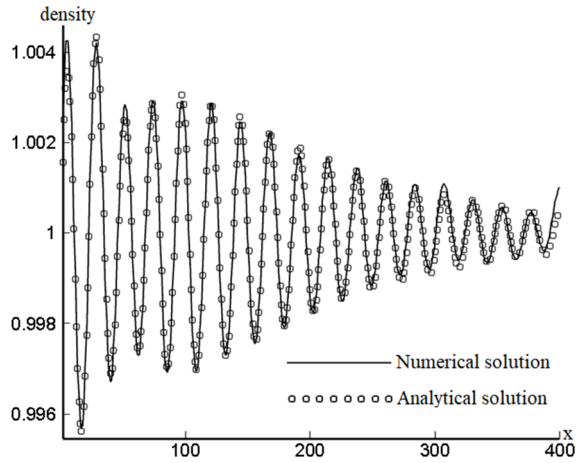

Figure 7: Longitudinal profiles of the analytical and numerical densities found after the improvement of the mathematical expression of the constant A (equation (12)).
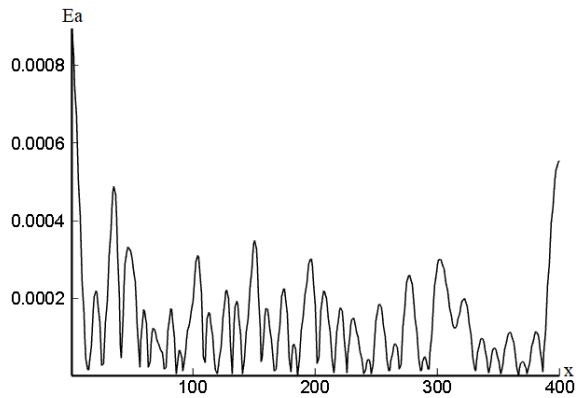

Figure 8: Oscillation of the absolute error between the analytical and numerical densities along the x-axis after the improvement of the mathematical expression of the constant A (equation (12)).

The analytical density field is shown in figure 9, in order to compare it with the numerical result shown in figure 4. There is a good resemblance between the two figures. Note, however, that due to the reflection of the waves due to the bounce-back boundary conditions applied in the numerical calculations, interferences occur and modify the waveform near the walls with regard to the analytically calculated density field. The reflected waves can be absorbed using the absorption boundary conditions, and this will be a future study.
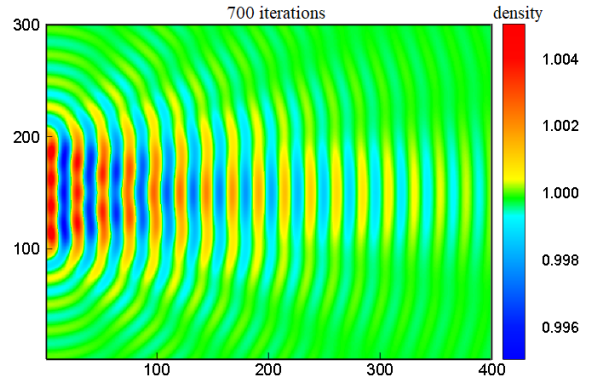

Figure 9: Analytical results found using the sum of the density expressed in equation (9) in the presence of the constant A formulated in equation (12).

5 CONCLUSIONS

This work deals with the simulation of acoustic waves using the MRT-LBM method. The numerical study presented here has shown that the LB method can be used to simulate the acoustic waves generated in air by a rectangular acoustic source. The proposed numerical model presents a good accuracy, confirmed by the comparison with the analytical calculation that is improved in this study compared to the one already reported in the literature. This validation is carried out using the mathematical expression of the density given by the wave equation solution for the case of cylindrical waves emitted by point sources (Benhamou et al., 2020).

REFERENCES

Bechereau, M. (2016). Élaboration de méthodes Lattice Boltzmann pour les écoulements bifluides à ratio de densité arbitraire (Doctoral dissertation).

Timm, K., Kusumaatmaja, H., Kuzmin, A., Shardt, O., Silva, G., and Viggen, E. (2016). The lattice Boltzmann method: principles and practice. Springer International Publishing AG Switzerland, ISSN, 1868-4521.

Mohamad, A. A. (2011). Lattice Boltzmann Method (Vol. 70). London: Springer.

Tristani, I. (2015). Existence et stabilité de solutions fortes en théorie cinétique des gaz (Doctoral dissertation, Paris 9).

Frisch, U., Hasslacher, B., and Pomeau, Y. (1986). Lattice-gas automata for the Navier-Stokes equation. Physical review letters, 56(14), 1505.

McNamara, G. R., and Zanetti, G. (1988). Use of the Boltzmann equation to simulate lattice-gas automata. Physical review letters, 61(20), 2332.

Frantziskonis, G. N. (2011). Lattice Boltzmann method for multimode wave propagation in viscoelastic media and in elastic solids. Physical Review E, 83(6), 066703.

O'Brien, G. S., Nissen-Meyer, T., and Bean, C. J. (2012). A lattice Boltzmann method for elastic wave propagation in a poisson solid. Bulletin of the Seismological Society of America, 102(3), 1224-1234.

Buick, J. M., Greated, C. A., and Campbell, D. M. (1998). Lattice BGK simulation of sound waves. EPL (Europhysics Letters), 43(3), 235.

Salomons, E. M., Lohman, W. J., and Zhou, H. (2016). Simulation of sound waves using the lattice Boltzmann method for fluid flow: Benchmark cases for outdoor sound propagation. PloS one, 11(1), e0147206.

Benhamou, J., Jami, M., Mezrhab, A., Botton, V., and Henry, D. (2020). Numerical study of natural convection and acoustic waves using the lattice Boltzmann method. Heat Transfer, 49(6), 3779-3796.

Marié, S., Ricot, D., and Sagaut, P. (2009). Comparison between lattice Boltzmann method and Navier–Stokes high order schemes for computational aeroacoustics. Journal of Computational Physics, 228(4), 1056-1070.

Weidong, S. H. A. O., and Jun, L. I. (2019). Review of Lattice Boltzmann Method Applied to Computational Aeroacoustics. Archives of Acoustics, 44(2), 215-238.

Guangwu, Y., Yaosong, C., and Shouxin, H. (1999). Simple lattice Boltzmann model for simulating flows with shock wave. Physical review E, 59(1), 454. Guangwu, Y., Yaosong, C., & Shouxin, H. (1999). Simple lattice Boltzmann model for simulating flows with shock wave. Physical review E, 59(1), 454.

Xiao, S. (2007). A lattice Boltzmann method for shock wave propagation in solids. Communications in numerical methods in engineering, 23(1), 71-84.

Moudjed, B. (2013). Caractérisation expérimentale et théorique des écoulements entrainés par ultrasons. Perspectives d'utilisation dans les procédés de solidification du silicium photovoltaïque (Doctoral dissertation, Lyon, INSA).

Sarvazyan, A. P., Urban, M. W., and Greenleaf, J. F. (2013). Acoustic waves in medical imaging and diagnostics. Ultrasound in medicine & biology, 39(7), 1133-1146.

Ranganayakulu, S. V., Rao, N. R., and Gahane, L. (2016). Ultrasound applications in medical sciences. IJMTER, 3, 287-93.

Viggen, E. M. (2009). The lattice Boltzmann method with applications in acoustics (Master's thesis, Norges teknisk-naturvitenskapelige universitet, Fakultet for naturvitenskap og teknologi, Institutt for fysikk).

Mezrhab, A., Moussaoui, M. A., Jami, M., Naji, H., and Bouzidi, M. H. (2010). Double MRT thermal lattice Boltzmann method for simulating convective flows. Physics Letters A, 374(34), 3499-3507.

Jami, M., Moufekkir, F., Mezrhab, A., Fontaine, J. P., and Bouzidi, M. H. (2016). New thermal MRT lattice Boltzmann method for simulations of convective flows. International Journal of Thermal Sciences, 100, 98-107.